Electron-Spin Manipulation and Resonator Readout in a Double-Quantum-Dot Nanoelectromechanical System

N. Lambert,[1,*] I. Mahboob,[2] M. Pioro-Ladrière,[3] Y. Tokura,[2,3] S. Tarucha,[4,3] and H. Yamaguchi[2]

[1]*Digital Materials Lab, Single Quantum Dynamics Research Group, FRS, Riken, Wako, Saitama 351-0198, Japan and Department of Basic Science, University of Tokyo, Komaba, Meguro-ku, Tokyo 153-8902, Japan*

[2]*NTT Basic Research Laboratories, NTT Corporation, Atsugi-shi, Kanagawa 243-0198, Japan*

[3]*Quantum Spin Information Project, ICORP, Japan Science and Technology Agency, Atsugi-shi, Kanagawa 243-0198, Japan*

[4]*Department of Applied Physics, University of Tokyo, Hongo, Bunkyo-ku, Tokyo, 113-0033, Japan*

(Received 18 December 2007; published 2 April 2008)

We demonstrate how magnetically coupling a nanomechanical resonator to a double quantum dot confining two electrons can enable the manipulation of a single electron spin and the readout of the resonator's natural frequency. When the Larmor frequency matches the resonator frequency, the electron spin in one of the dots can be selectively and coherently flipped by the magnetized oscillator. By simultaneously measuring the charge state of the two-electron double quantum dots, this transition can be detected thus enabling the natural frequency and displacement of the mechanical oscillator to be determined.

DOI: 10.1103/PhysRevLett.100.136802 PACS numbers: 73.21.La, 62.25.Jk, 72.25.Dc

Quantum dots are artificial atoms which enable the confinement of a few, or even one, electron [1]. In these devices, the spin of the individual electron forms a natural two-level system and provides great potential for the realization of a solid-state qubit, with applications in spintronics and quantum information schemes [2]. However, successful realization of these proposals requires efficient, fast, and *selective* control of the electron spin state [3,4]. In this regard, coherent spin manipulation in a double quantum dot has been recently demonstrated by utilizing a variety of mechanisms, including rapid electrical control of the exchange interaction [3], by generating a local electron spin resonance (ESR) magnetic field [4], and by coupling the electron spin to nuclear hyperfine or spin-orbit fields [5,6].

Here we present a novel scheme for magnetically coupling a nanoelectromechanical resonator [7–10] to the spin of *one of two* electrons confined within a double quantum dot (DD) device. An oscillating magnetic field (ESR field) in one plane is produced by the oscillations of the magnetized resonator, while a static field with a strong gradient is produced in another plane (providing Zeeman splitting). The oscillating field selectively couples to one of the electrons, and the corresponding change in the two-electron spin state is then detected by spin blockade charge sensing [3,4,11]. We model the interaction with a master equation approach, to include both spin decay and spin dephasing processes (via nuclear hyperfine fields). We show that this mechanically induced ESR process is advantageous, as it only requires a weak external tuning field, and no rapid electrical AC fields. In addition, our scheme also enables the resonator's natural frequency to be measured, and its displacement to be transduced, illustrating that the electron spin can be used as a sensitive quantum displacement detector.

Device geometry and parameters.—We begin with a schematic of the proposed coupled nanomechanical resonator (NEM) DD system, and corresponding parameters, shown in Fig. 1. A GaAs/AlGaAs nanomechanical beam is located distance d_0 from the mesa on which the DDs reside. The natural frequency for a resonator of these dimensions is expected to be 200 MHz with peak displacement, at the center of the beam, of $\sim$5 nm with an achievable quality factor of 10^4. The beam will be actuated to resonance via the piezoelectric effect between the Schottky gate and the 2DES located above the beam clamping point [12]. An actuation voltage of <10 mV_{rms} is necessary to excite the beam to resonance, where the resulting parasitic

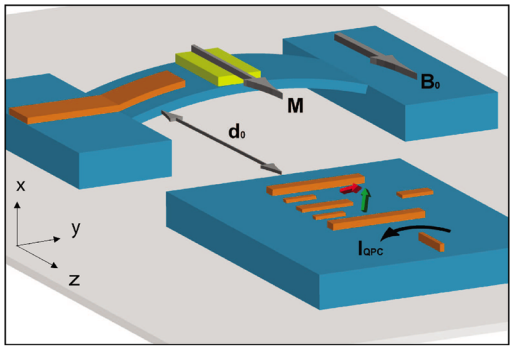

FIG. 1 (color online). A schematic of the proposed coupled mechanical resonator double QD system. The mechanical oscillator is a suspended doubly clamped beam located a distance d_0 from the mesa on which the double QDs are defined via electrostatic gates. A micromagnet of magnetization M is incorporated onto the beam oscillator and moves in unison with the out of plane beam motion. The mechanical oscillator couples to the confined electron spins (small arrows) in the double QDs via the micromagnet's stray magnetic field where the degree of coupling is controlled by the external tuning field B_0.

electric field is too small to perturb the DD system. The double dots are defined using electrostatic gates on the surface of the heterostructure where the 2DEG is located typically 100 nm below the surface [13].

The resonator is coupled to the DDs magnetically by placing a Co micromagnet on the resonator, without impairing the resonance [14], as depicted in Fig. 1, with $\mu_0 M = 1.8$ T, where μ_0 and M are the permeability of free space and magnetization of Co, respectively. The Co micromagnet is engineered so that the magnetization vector remains parallel to the easy axis for small values ($\sim$50 mT) of the external tuning field, B_0. The micromagnet can be realized via routine lithographic processes where a single domain of high magnetization is required for this scheme.

The left and right dots are located distances $d_1 = 150$ nm and $d_2 = 250$ nm from the mechanical resonator, respectively. Under these conditions, with the nanomechanical beam at resonance, the total field, including an external tuning field B_0, is of the form $B_n = [B_0 + B_{zn} + \delta B_{zn} \sin(\omega_r t)]\hat{\mathbf{z}} - B_{xn} \sin(\omega_r t)\hat{\mathbf{x}}$. The stray field of the Co micromagnet has been calculated analogously to the method outlined in Ref. [15]. The in-plane (Zeeman) magnetic field B_z arising from the above described magnetic element is shown in Fig. 2(a). At the quantum dot (QD) locations, the in-plane magnetic field at the left (right) dot is $B_{z1(2)} = 94$ mT (36 mT).

The proximity of the magnetic element to the DDs produces a strong in-plane field gradient of order $(B_{z1} - B_{z2})/(d_1 - d_2) \sim 0.6$ T/μm, which allows the nanomechanical oscillator to addressably couple to the electron spin in either quantum dot as discussed below. The spatial dependence of the transverse magnetic field $B_x^{\max}$ while the beam is at maximum deflection is shown in Fig. 2(b). In the inset of Fig. 2(b), the time dependence of the transverse magnetic field B_x at the locations of the DDs while the beam is at resonance is shown. The amplitude of this field at the location of the left (right) dot is $\sim$3.0 mT (0.8 mT) which is more than sufficient to flip the electron spin in either dot via ESR. As can be seen from Figs. 2(a) and 2(b), the parameter $d_0 \approx 50$ nm is of critical importance as this governs the degree to which the DDs couple to the resonator via the magnetic element and can be achieved via state of the art electron beam lithography. In summary, the magnetized resonator provides a weak oscillating field in the x direction, and a static field in the z direction with a large gradient between the two dots. This is in contrast to Ref. [15] where ESR is implemented via the dynamical motion of the electron in the *static* stray field of the micromagnet.

Hamiltonian.—For two-electron QDs, the relevant spin states are the spin singlet and triplet states of the (1,1) charge state ($|S\rangle, |T_0\rangle, |T_+\rangle, |T_-\rangle$) and the spin singlet of the (0,2) charge state [$|(0,2)S\rangle$] where the label (m, n) refers to the number of electrons confined on the left and right dots [16]. In the presence of finite interdot

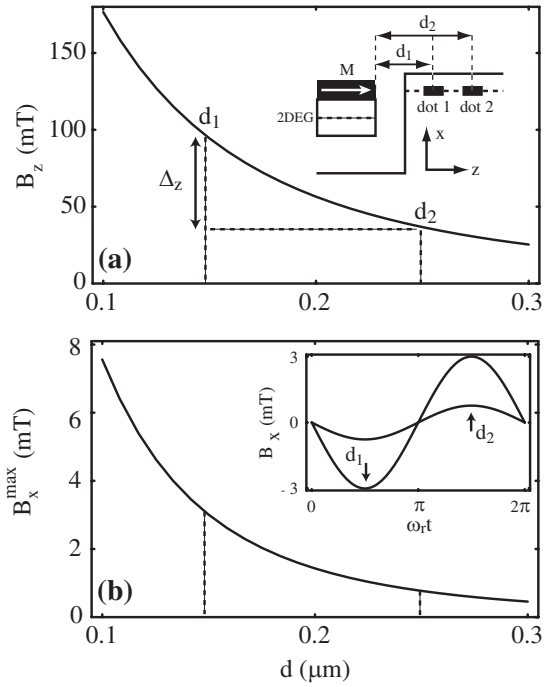

FIG. 2. (a) The profile of the in-plane (Zeeman) magnetic field B_z near the nanomechanical resonator with external tuning field $B_0 = 0$ T, where d_1 and d_2 mark the positions of the left and right quantum dots, respectively. The inset shows the cross section of the proposed system. (b) The profile of the transverse magnetic field $B_x^{\max}$ while the resonator is at maximum deflection (5 nm). The inset shows the time dependence of the ESR field at the positions of the quantum dots while the mechanical element is at resonance.

tunnelling T the (1,1) and (0,2) singlets are coupled allowing electrons to be moved between dots when the detuning parameter ϵ is varied (by pulsing the QD gate voltages). The energy $\Delta_z = g\mu_B(B_{z1} - B_{z2})/2$ couples the $|S\rangle$ and $|T_0\rangle$ states while $|T_+\rangle$ and $|T_-\rangle$ remain eigenstates with Zeeman energy $E_Z = \pm g\mu_B(B_{z1} + B_{z2} + 2B_0)/2$, where g is the electron g factor ($|g| = 0.44$ for GaAs) and μ_B is the Bohr magneton. For the *stationary resonator*, the Hamiltonian describing the two-electron states in the presence of the above described in-plane inhomogeneous magnetic field in the $\{|(0,2)S\rangle, |S\rangle, |T_0\rangle, |T_+\rangle, |T_-\rangle\}$ basis is $H = -\epsilon|(0,2)S\rangle\langle(0,2)S| + \sqrt{2}T(|(0,2)S\rangle\langle S| + \text{c.c.}) - \Delta_z(|S\rangle\langle T_0| + \text{c.c.}) - E_Z|T_+\rangle\langle T_+| + E_Z|T_-\rangle\langle T_-|$.

In Fig. 3(a), the eigenenergies of H are plotted as the detuning is swept between the (1,1) and (0,2) charge states across the degeneracy point ($\epsilon = 0$). For large positive detuning, the ground state is $|(0,2)S\rangle$. Close to $\epsilon = 0$, T and Δ_z mix the $|(0,2)S\rangle$, $|S\rangle$, and $|T_0\rangle$ states. For large negative ϵ, $|(0,2)S\rangle$ uncouples from $|S\rangle$ and $|T_0\rangle$ to become the highest energy state. In the absence of a field gradient ($\Delta_z = 0$), $|S\rangle$ and $|T_0\rangle$ would also be eigenstates with splitting equal to the exchange energy $J \approx T^2/\epsilon$. However, because $\Delta_z \gg J$, the actual eigenstates are the superpositions $[(|S\rangle \pm |T_0\rangle)/\sqrt{2}]$ which correspond to the states $|\uparrow\downarrow\rangle$ (spin up and spin down at the left and right QDs,

respectively) and $|\downarrow\uparrow\rangle$, respectively. Moreover, the field gradient in the regime of large negative detuning results in asymmetric separation of $|T_+\rangle$ and $|T_-\rangle$ states about $|\uparrow\downarrow\rangle$, where the energetic separation between the $|\uparrow\downarrow\rangle$ and $|T_+\rangle = |\uparrow\uparrow\rangle$ states is $\Sigma_{z2} = g\mu_B(B_0 + B_{z2})$, the Zeeman energy of the right spin.

Spin isolation and ESR.—The nanomechanical resonator can be used to manipulate the electron spin states in the DDs as follows. The resonator is excited at its natural frequency corresponding to an energy $\hbar\omega_r$; the equivalent magnetic field $\hbar\omega_r/g\mu_B$ is designed to be much greater than GaAs hyperfine magnetic field $B_N \sim 1$ mT. The in-plane tuning magnetic field ($B_0 = -3.5$ mT here) is then used to adjust the Zeeman spin splitting to couple the right QD and the mechanical element by setting $\Sigma_{z2} = \hbar\omega_r$. With the mechanical element at resonance, the $|(0, 2)S\rangle$ state is prepared (A) which is then separated into the $|\uparrow\downarrow\rangle$ state by the in-plane magnetic field gradient between the two QDs and by using rapid adiabatic passage to change ϵ from a positive to a negative value ($A \rightarrow B$) [13]. With the right QD resonantly coupled to the resonator, the transverse ESR magnetic field couples only the $|\uparrow\downarrow\rangle$ and $|T_+\rangle$ states at a rate proportional to $\Sigma_{x2} = g\mu_B B_{x2}$.

The coupled system is held in this state for time τ_{ESR} until a steady state has been achieved ($B \rightarrow C$). After manipulation, rapid adiabatic passage is used to change ϵ from negative to positive values for a charge sensing measurement via the quantum point contact, QPC ($C \rightarrow D$). The $|(1, 1)T_+\rangle$ state remains in the spin-blocked configuration whereas the $|\uparrow\downarrow\rangle$ tunnels directly to $|(0, 2)S\rangle$ [Fig. 3(b)]. After manipulation, the spin state is a mixture of $|(0, 2)S\rangle$ and $|(1, 1)T_+\rangle$ states (at point D). In this condition, the QPC current I_{QPC} will be a mixture of the corresponding (0,2) and (1,1) charge states. At off resonance, the spin configuration at (D) will be $|(0, 2)S\rangle$ with a (0,2) QPC signal. Therefore, by sweeping the tuning field across resonance, a peak in the I_{QPC} is expected.

Master equation of ESR Hamiltonian.—During the period where the right dot is coupled to the resonator, the left spin can be neglected, and the Hamiltonian becomes

$$H_{\mathrm{ESR}} = -\Sigma_{z2}\sigma_{z2}/2 + \Sigma_{x2}(\omega_r, \omega_d, Q)\sin(\omega_d t)\sigma_{x2}/2, \quad (1)$$

where $\sigma_{n2} = (\sigma_{x2}, \sigma_{y2}, \sigma_{z2})$ are the Pauli matrices of the spin located in the right QD, ω_r is the natural frequency of the resonator, and ω_d is the driving frequency of the resonator. To robustly model the coupled system, the various mechanisms by which the electron spins can decohere must be considered. Elsewhere it has been shown that the hyperfine interaction of the electron spin with nuclear spins within the quantum dots [17] dominates, causing T_2 times of the order of nanoseconds. In contrast, spin-orbit coupling [18] produces T_1 times of milliseconds.

Under these conditions, the master equation describing the spin states of the electron in the right dot is

$$\frac{d\rho(t)}{dt} = -(i/\hbar)[H_{\mathrm{ESR}} + H_N, \rho(t)] + L[\rho(t)], \quad (2)$$

where $H_N = -g.\mu_B(B_N.\sigma_2)$ is the hyperfine interaction and $L[\rho(t)]$ describes the incoherent Markovian spin relaxation at rate γ (since $T_1 = 1$ ms, we take $\gamma = 1$ kHz). We reach the steady state solution by taking $t \rightarrow \infty$, $\frac{d\rho(t)}{dt} = 0$, and thus inverting to find $\rho(t \rightarrow \infty) = \{(-i/\hbar)[H_{\mathrm{ESR}} + H_N, \rho(t)] + L\}^{-1}$. Assuming the rotating wave approximation, we are able to obtain an analytical solution for the occupation of the $|(1, 1)T+\rangle$ and $|(0, 2)S\rangle$ states.

For static hyperfine nuclear fields B_N, the steady state of the density matrix elements for the diagonal $|(1, 1)T_+\rangle$ state is

$$\rho_{(1,1)T_+} = [16B_{Y,N}^2 + (4B_{X,N} + \Sigma_{x2})^2]/[32B_N^{(2)} + 32\Sigma_{x2}B_{X,N} + 64\hbar B_{Z,N}\Delta\omega + 2\Sigma_{x2}^2 + \hbar^2(16\Delta\omega^2 + 4\gamma^2)] \quad (3)$$

and $\rho_{(0,2)S} = 1 - \rho_{(1,1)T_+}$ where $B_N^{(2)} = (B_{X,N}^2 + B_{Y,N}^2 + 2B_{Z,N}^2)$, $\Delta\omega = \Sigma_{z2}/\hbar - \omega_d$ is the detuning, and $B_{i,N}$ is the nuclear field in the ith direction. We assume that the

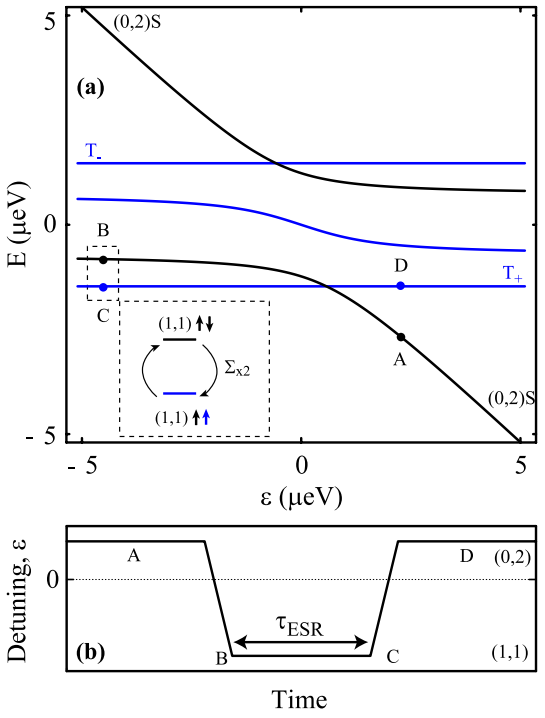

FIG. 3 (color online). (a) The two-electron spin states as a function of detuning energy with interdot tunnelling, $\sqrt{2}T = 1$ μeV with the external tuning field set to zero. At large negative detuning, the transverse ESR field (B_{x2}) resonantly couples the $|\uparrow\downarrow\rangle$ and $|T_+\rangle$ states (horizontal lines) when the condition $g\mu_B(B_{z2} + B_0) = \hbar\omega_r$ is satisfied. (b) The pulse sequence consisting of preparation in the $|(0, 2)S\rangle$ (A), resonant coupling of the $|\uparrow\downarrow\rangle$ and $|T_+\rangle$ states for time τ_{ESR} ($B \rightarrow C$) and readout (D) steps. For $\tau_{\mathrm{ESR}} = \tau_\pi$, the final state at point (D) is the triplet $|T_+\rangle$.

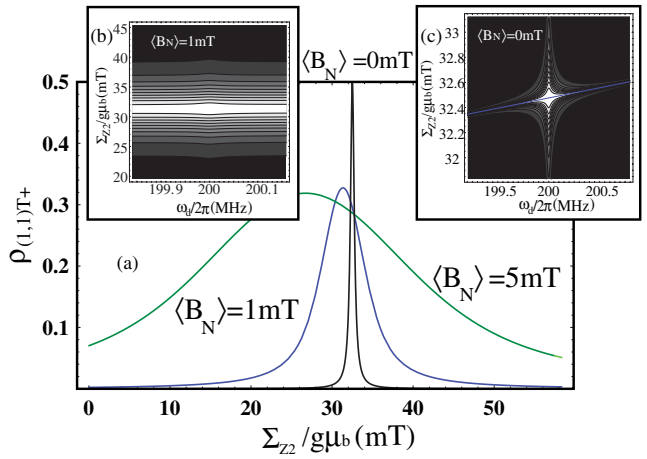

FIG. 4 (color online). (a) QPC response/occupation of the $|(1,1)T_+\rangle$ state as a function of the field $\Sigma_{z2}/g\mu_B$. The resolution of the ESR peak is reduced and broadened by the increasingly strong nuclear field. The range of fields presented here are $\langle B_N\rangle = 0$, 1, 5 mT, with the expected hyperfine field in GaAs being 1 mT. (b) Contour plot of the $|(1,1)T_+\rangle$ state for $\langle B_N\rangle =$ 1 mT. There remains a broadened response when $\omega_r = \omega_d$, identifying the natural frequency of the resonator. (c) Again a contour plot of the $|(1,1)T_+\rangle$ state, but now for $\langle B_N\rangle = 0$ mT. There is a double Lorentz structure around $\omega_d = \omega_r$ and $\omega_d = \Sigma_{z2}/\hbar$. Here, white is maximum [0.42 for (b), 0.5 for (c)], black is minimum.

nuclear field is static on the $\hbar/\Sigma_{x2}$ and $1/\gamma$ time scales, but is fast on the time scale of collating a clear QPC measurement.

Thus, in the calculation presented in Fig. 4, we integrate over a normal distribution of possible nuclear spin orientations [19,20] with mean value $\langle B_N\rangle = \sqrt{3}\langle B_{i,N}\rangle$, and a standard deviation of $\sqrt{2}\langle B_N\rangle$, so

$$\rho^{B_N}_{(1,1)T_+} = \int_{-\infty}^{\infty} dB_{i,N}\rho_{(1,1)T_+}\prod_{i=x,y,z}\frac{e^{\{[-(B^2_{i,N}-\langle B^2_{i,N}\rangle)^2/4\langle B_{i,N}\rangle^2]\}}}{(2\langle B_{i,N}\rangle\sqrt{\pi})}. \quad (4)$$

Consequently, $\langle B_N\rangle$ is the important quantity in determining the effect of the nuclear field on the ESR measurement. In Fig. 4, the effects of the hyperfine coupling on the QPC measurement are shown. For $\langle B_N\rangle < \Sigma_{x2}$ the on resonance response of the QPC is clearly visible. For $\langle B_N\rangle \geq \Sigma_{x2}$ the on resonance peak becomes smeared out and eventually obliterated.

ESR line width and displacement detection.—In the H_{ESR} Hamiltonian, the magnitude of the Σ_{x2} is proportional to the displacement of the resonator $\Sigma_{x2}(\omega_r, \omega_d, Q) = Cx(\omega_r, \omega_d, Q) = CF/\sqrt{m(\omega_r^2 - \omega_d^2)^2 + 4\omega_r^2\omega_d^2/(Q^2)}$, where C is a proportionality constant of 0.16 mT as derived in [15] and $x(\omega_r, \omega_d, Q)$ is the driven harmonic oscillator response function for the resonator with effective mass m driven with a force F. If we assume the hyperfine interaction and the stochastic decoherence rate of the spin are weak ($\gamma = 0$) the ESR response is $\rho_{(1,1)T_+} = \frac{1}{2}(1 + \frac{2\hbar^2}{\Sigma_{x2}^2\Delta\omega^2})$. When the resonator is driven at resonance $\omega_d = \omega_r$, the line width of this response is $\gamma_{\mathrm{ESR}} = \Sigma_{x2}/2$. Assuming adequate resolution, the line width immediately gives us a direct transduction of the displacement of the oscillator, in that $x_{\max} = 2\gamma_{\mathrm{ESR}}/C$.

Finally, when driving the resonator off resonance the field Σ_{x2} is itself a Lorentzian around $\omega_d = \omega_r$. Thus, observing the ESR response in the full ω_d and Σ_{x2} spectra shows a Lorentzian form with two maxima [Fig. 4(c)].

Conclusions.—We have shown that magnetically coupling the spin of an electron confined in a double quantum dot to a high frequency nanomechanical resonator produces selective and coherent rotations of the electron spin. The electron spin state can then be read out from a QPC measurement using spin blockade. Simultaneously we have shown that the electron spin acts as a highly sensitive quantum detector, which allows the maximum displacement of the resonator, and its natural frequency, to be detected.

We acknowledge financial support from the Grant-in-Aid for Scientific Research A (No. 40302799), the Special Coordination Funds for Promoting Science and Technology, MEXT, SORST-JST, DARPA Grant No. DAAD19-01-1-0659 of the QuIST program, JSPS KAKENHI (Grant No. 16206003), and JSPS Grant No. 17-05761.

*nwlambert@riken.jp

[1] R. C. Ashoori, Nature (London) **379**, 413 (1996).
[2] D. Loss and D. P. DiVincenzo, Phys. Rev. A **57**, 120 (1998).
[3] J. Petta *et al.*, Science **309**, 2180 (2005).
[4] F. H. L. Koppens *et al.*, Nature (London) **442**, 766 (2006).
[5] E. A. Laird *et al.*, Phys. Rev. Lett. **99**, 246601 (2007).
[6] K. C. Nowack *et al.*, Science **318**, 1430 (2007).
[7] H. G. Craighead, Science **290**, 1532 (2000).
[8] A. Cho, Science **299**, 36 (2003).
[9] M. Roukes, Phys. World **14**, 25 (2001).
[10] P. Treutlein *et al.*, Phys. Rev. Lett. **99**, 140403 (2007).
[11] J. M. Elzerman *et al.*, Nature (London) **430**, 431 (2004).
[12] I. Mahboob and H. Yamaguchi (unpublished).
[13] J. M. Elzerman *et al.*, Phys. Rev. B **67**, 161308(R) (2003).
[14] D. Rugar *et al.*, Nature (London) **430**, 329 (2004).
[15] M. Pioro-Ladrière *et al.*, Appl. Phys. Lett. **90**, 024105 (2007).
[16] J. M. Taylor *et al.*, Nature Phys. **1**, 177 (2005).
[17] W. A. Coish and D. Loss, Phys. Rev. B **72**, 125337 (2005).
[18] A. V. Khaetskii and Y. V. Nazarov, Phys. Rev. B **64**, 125316 (2001).
[19] F. H. L. Koppens *et al.*, J. Appl. Phys. **101**, 081706 (2007).
[20] I. A. Merkulov, A. L. Efros, and M. Rosen, Phys. Rev. B **65**, 205309 (2002).